International Journal of Medical Science and Clinical Research Studies

ISSN(print): 2767-8326, ISSN(online): 2767-8342

Volume 03 Issue 10 October 2023

Page No: 2507-2513

DOI: https://doi.org/10.47191/ijmscrs/v3-i10-72, Impact Factor: 6.597

A Conceptual Design of a Novel Multi-Hexagonal Beta Applicator Intended to Treat Non-Melanoma Skin Cancers

Eduardo De Paiva

Division of Medical Physics, Institute of Radiation Protection and Dosimetry Rio de Janeiro, Brazil

ABSTRACT

Due to its short range in tissue and high dose gradient beta radiation may be used to the therapy of small and superficial skin lesions. In this short study a conceptual design of a novel multi-hexagonal beta applicator loaded with Yttrium-90 is presented. Calculations of dose rates around the applicator area performed using the beta-point source dose function formalism and initial results show that over 90\% of the beta radiation energy from the multi-hexagonal applicator loaded with Yttrium-90 is absorbed in the first layers of the skin tissue. Results show that the multi-hexagonal beta applicator has the potential to be used in the brachytherapy treatment of non-melanoma skin cancers.

KEYWORDS: beta radiation, Yttrium-90, dose distributions, multi-hexagonal beta applicator, brachytherapy, non-melanoma skin cancer

ARTICLE DETAILS

Published On:
30 October 2023

Available on:
https://ijmscr.org/

INTRODUCTION

Non-melanoma skin cancers are among the most common types of cancer in the world, and the number of new cases is expected to continue to increase in the coming years, mainly due to the global increase in life expectancy and the growing popularity of tanning [1]. A characteristic of non-melanoma skin cancers is that they usually develop in the most external layers, and the most common are basal cell carcinoma and cutaneous squamous cell carcinoma. Treatment of non-melanoma skin cancers depend on its size, location and type, and the most common kind of treatment is by means of the Mohs micrographic surgery, which is the gold-standard to treat high-risk non-melanoma skin cancers [2]. However, due to various reasons, Mohs surgery may not be available, and the management of non-melanoma skin cancers may be performed by other types of therapies. Alternative therapies may include chemotherapy, electrodessication and curettage, cryosurgery, photodynamic therapy, and radiation therapy [2].

Radiotherapy using external high energy photons or particles produced in large medical accelerators may be used to the management of non-melanoma skin cancers. Brachytherapy treatment technique, where the radiation source is placed near or in contact with the tumor, may be also used to treat non-melanoma skin tumors [3-12]. Regardless of the radiation technique used the success of treatment depends on delivering a conformal dose to the target volume while sparing the healthy surrounding tissues. In this sense, conformal beta applicators play an important role in the treatment of skin cancers [3-6,8,9,11,12].

High-energy beta particles emitted from certain unstable nuclei have important medical applications in the brachytherapy treatment of various diseases, and in particular in the treatment of skin cancers [13-19]. Two features make the beta particles suitable to be used in the brachytherapy treatment of small and superficial skin lesions; first, their short range in tissue, since that the healthy structures beyond the lesion can be spared [7,9,11] second, the simple radiation protection procedures on handling the beta sources, since the material of the beta applicator (or plaque) is sufficient to stop the beta particles in the unwanted direction. However, a great problem in the use of beta particles in medicine is the experimental measurement of beta radiation dose distributions in tissue mainly due to the sharp dose gradient and short range of the beta particles. In this sense theoretical calculation methods of dose distributions around beta applicators play an important role [5,7,9,12,15].

In this work we propose a novel multi-hexagonal shaped beta applicator designed

and intended to be used in the treatment of non-melanoma skin cancers, as shown in Figure 1. Its multi-hexagonal shape can aid to deliver conformal radiation dose distributions to the non-melanoma skin lesion. A first insight into dose distributions around the conceptual multi-hexagonal beta applicator based on an analytical/numerical method is presented for the applicator loaded with the Yttrium-90 radionuclide.

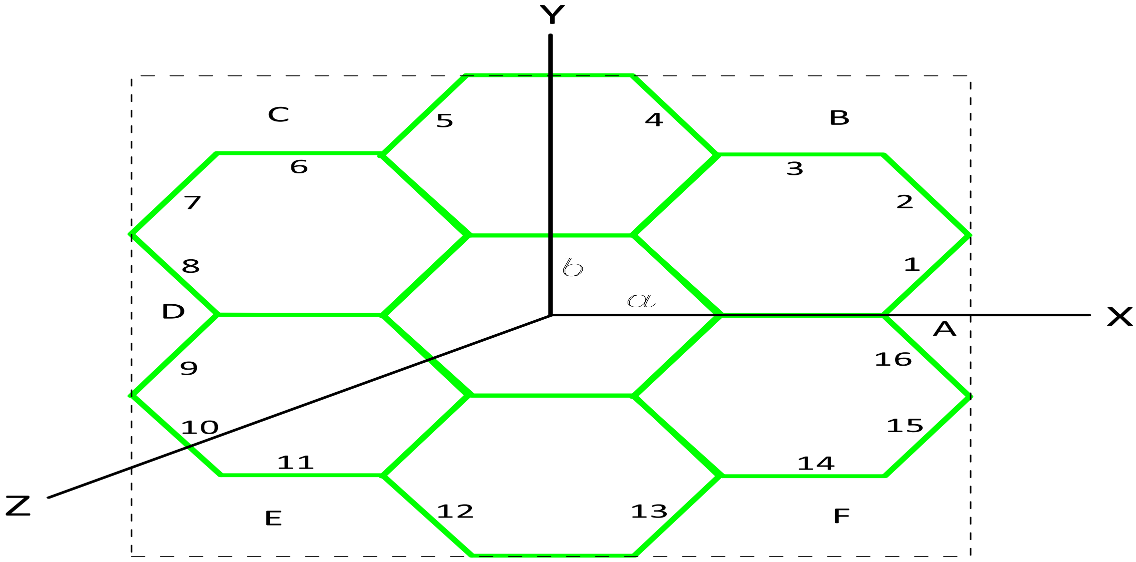

Figure 1. The geometry of the conceptual multi-hexagonal beta applicator. All the 7 hexagons have side a and inradius b. The applicator is inscribed in a rectangle of dimensions $5a$ x $6b$, with $b = \frac{a}{2}\sqrt{3}$. A to F are external regions of the applicator and numbers 1 to 16 are line segments as described in the text.

METHODS

A simple approach used to estimate the radiation dose distributions around beta sources consist of determining a simple mathematical expression to represent the dose distribution around a beta point-source (or point kernel) and then integrating it over the total area or volume of the extented source. This method, the beta-point source dose formalism, was developed by Loevinger [20] based on available experimental dose distributions in air and theoretical studies on absorbed dose distributions around point sources of beta emitting nuclides, and later modified by Vynckier and Wambersie considering a new set of data [21,22]. The beta-point source dose function is given by a relatively simple expression

,

$$J(\xi) = \frac{B}{(\rho\upsilon\xi)^2}\left\{c\left[1 - \frac{\rho\upsilon\xi}{c}\exp\left(1 - \frac{\rho\upsilon\xi}{c}\right)\right] + \rho\upsilon\xi exp(1 - \rho\upsilon\xi) - \rho\upsilon\xi\left(1 - \frac{\rho\upsilon\xi}{2} - \frac{f}{2}\right)\right\}, \qquad (1)$$

Here $J(\xi)$ is the beta-point dose function given at a distance ξ from the point-source [21,22]. The quantity B is a normalization constant obtained by considering that the total energy per disintegration, absorbed in a very large sphere, is equal to the energy emitted. B is written as

$$B = \frac{0.046\rho^2\upsilon^3\overline{E}_\beta}{3c^2 - (c^2 - 1)\exp(1) + (3 + f)\exp(1 - f) - 4\exp\left(1 - \frac{f}{2}\right)}, \qquad (2)$$

where c and f are dimensionless parameters; ρ is the medium density; υ is the absorption coefficient, and ($\overline{E}_\beta$ is the mean kinetic energy of the beta particles.

The dimensionless parameter f in (1) was introduced by Vynckier and Wambersie [21,22] to include a set of theoretical and experimental data not previously used by Loevinger [20], and $f/\rho\upsilon$ accounts for the distance from which the dose due to beta radiation is required to be zero due to the short range of the beta radiation,

$$J(\xi) \equiv 0, \quad \text{for} \quad \rho\upsilon\xi \geq f. \qquad (3)$$

Also, in Equation (1) the term within the braces accounts for the energy absorbed from the unscattered component of the beta particles and is negligible at distances beyond $c/\rho\upsilon$,

$$\left[1 - \frac{\rho\upsilon\xi}{c}exp\left(1 - \frac{\rho\upsilon\xi}{c}\right)\right] \equiv 0, \quad \text{for} \quad \rho\upsilon\xi \geq c. \qquad (4)$$

The absorbed dose rate $\dot{D}$ from an extended beta source at given point of interest $P_0(x_0, y_0, z_0)$ is obtained by summing up the contribution of all points in the multi-hexagonal applicator (see Figure 1),

$$\dot{D} = a_S \iint J(\xi).\,dS, \qquad (5)$$

where a_S is the superficial activity and dS is the area element. The distance from a point on the plaque to a point of interest P_0 on the medium (tissue) is

$$\xi = \sqrt{(x - x_0)^2 + (y - y_0)^2 + z_0^2}. \qquad (6)$$

The dose rate at a given depth z_0 is obtained by numerical integration of (5) for the $5a$ x $6b$ rectangle but excluding the regions from A to F, as shown in Figure 1. Numerical integrations were carried out using a code written in Fortran language, and within the code points located above the line segments:

$$y_2 = 6b - \frac{2b}{a}x \qquad (7)$$

$$y_3 = 2b \qquad (8)$$

$$y_4 = 4b - \frac{2b}{a}x \qquad (9)$$

$$y_5 = 4b + \frac{2b}{a}x \qquad (10)$$

$$y_6 = 2b \qquad (11)$$

$$y_7 = 6b + \frac{2b}{a}x \qquad (12)$$

$$y_9 = 4b + \frac{2b}{a}x \qquad (13)$$

$$y_{16} = 4b - \frac{2b}{a}x, \qquad (14)$$

and below the line segments:

$$y_1 = -4b + \frac{2b}{a}x \qquad (15)$$

$$y_8 = -4b - \frac{2b}{a}x \qquad (16)$$

$$y_{10} = -6b - \frac{2b}{a}x \qquad (17)$$

$$y_{11} = -2b, \qquad (18)$$

$$y_{12} = -4b - \frac{2b}{a}x \qquad (19)$$

$$y_{13} = -4b + \frac{2b}{a}x \qquad (20)$$

$$y_{14} = -2b, \qquad (21)$$

$$y_{15} = -6b + \frac{2b}{a}x, \qquad (22)$$

are discarded to consider only the multi-hexagon.

RESULTS AND DISCUSSION

Let us consider in this study a multi-hexagon of sides equal to 0.5 cm loaded with the Yttrium-90 radioisotope (half-life equal to 64.1 hours, and maximum kinetic energy of the beta particle equal to 2.28 MeV) uniformly distributed on the surface of the applicator. We also consider the plaque as having a constant activity of 1 MBq/cm^2. The parameters c, f, υ and $\overline{E}_\beta$ are respectively 0.95, 4.48, 5.05 cm^2/g and 0.933 MeV for 90-Y [9].

In Figure 2 are depicted the results of dose rates against the depth along central z-axis in tissue. Results are normalized at the 1 mm depth and clearly show a strong decrease of doses at a very short distances from the surface of the applicator. Doses decrease to 50% of the reference value at 2 mm depth; 20% at 3.5 mm depth; 10% at 4.5 mm depth and tend to zero from 7 mm on. These results emphasize the short-range nature of beta particles and their useful application in the treatment of small and superficial skin lesions [3-12].

In Figure 3 are displayed the normalized dose rates along the lateral x-axis at five different depths from 1 to 5 mm for the multi-hexagonal Yttrium-90 beta applicator. It can be observed that near the surface of the applicator there is a strong fall off of doses as distances from the center of applicator increase. At 1 mm depth dose rates are nearly equal to 1 for lateral distances less than 5 mm; the doses drop to about 50% for lateral distance around 10.6 mm and are negligible from lateral distances equal to 17 mm on. At 3 mm depth the dose rates are nearly equal to 28% for lateral distances up to 6 mm; doses are 14% at lateral distance equal to 11 mm, and they are negligible from 15 mm on. At 5 mm depth the maximum dose rate is 6.75% of the reference dose, and doses are negligible for further depths.

In Figure 4 are shown the normalized dose rates along the lateral y-axis at five different depths, from 1 to 5 mm. Also, again it can be observed that near the surface of the Yttrium-90 beta applicator doses decrease strongly as distances from the center of applicator increase. At 1 mm depth dose rates are nearly equal to 1 for lateral distances less than 6.5 mm; the doses drop to about 50% for lateral distance around 12.7 mm and are negligible from lateral distances equal to 18

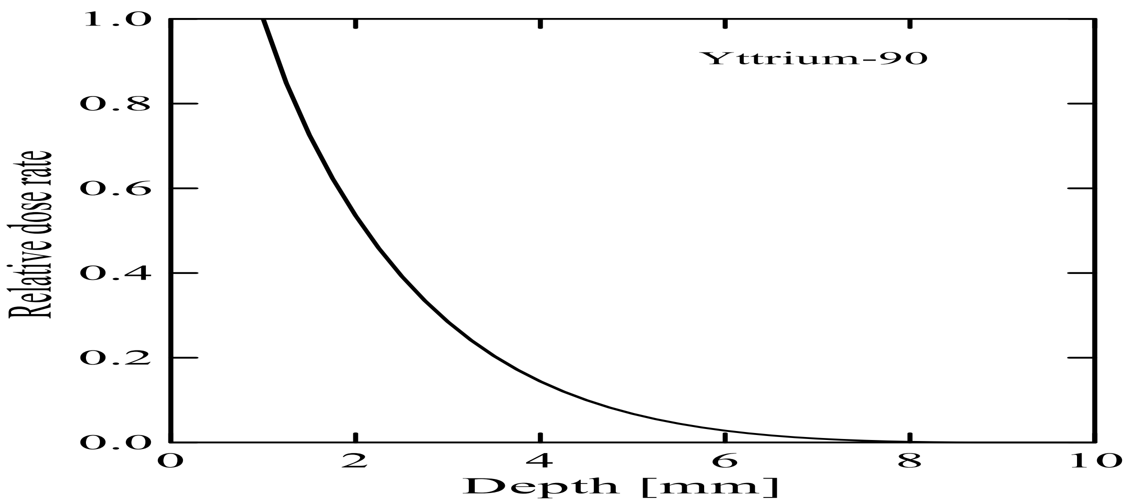

Figure 2. Depth-doses along central axis of the multi-hexagonal Yttrium-90 beta applicator obtained by integration of the beta-point source dose function over its total area. Results are normalized at 1 mm depth.

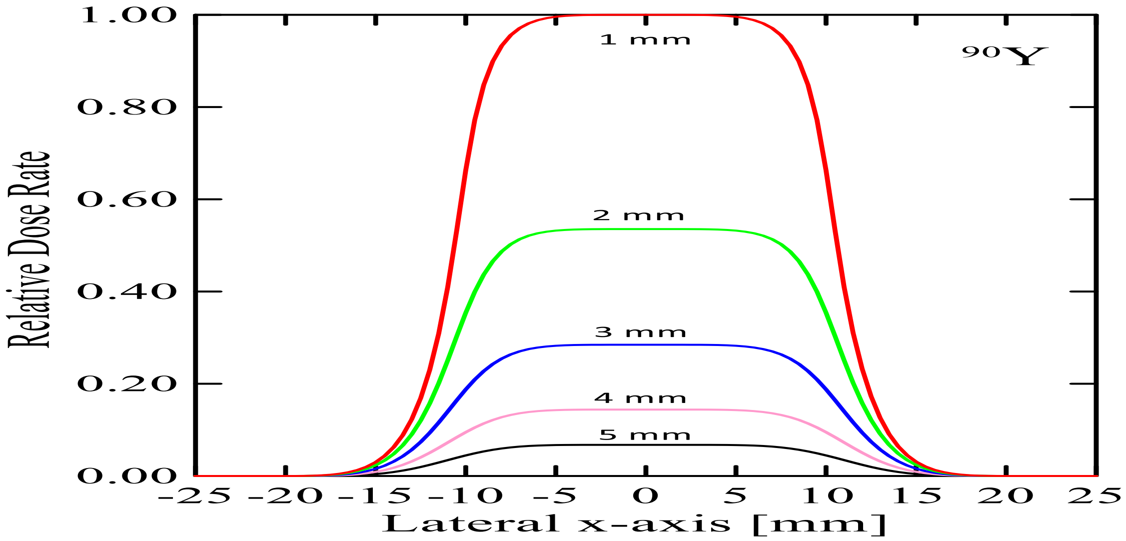

Figure 3. Relative lateral dose rates along *x*-axis for the multi-hexagonal Yttrium-90 beta applicator at 1-, 2-, 3-, 4- and 5-mm depths.

mm on. At 3 mm depth the dose rates are nearly equal to 28% for lateral distances up to 6.5 mm; doses are 14% at lateral distance equal to 12.5 mm, and they are negligible from 17 mm on. At 5 mm depth the maximum dose rate is also 6.75% of the value of reference, and doses are negligible for greater depths.

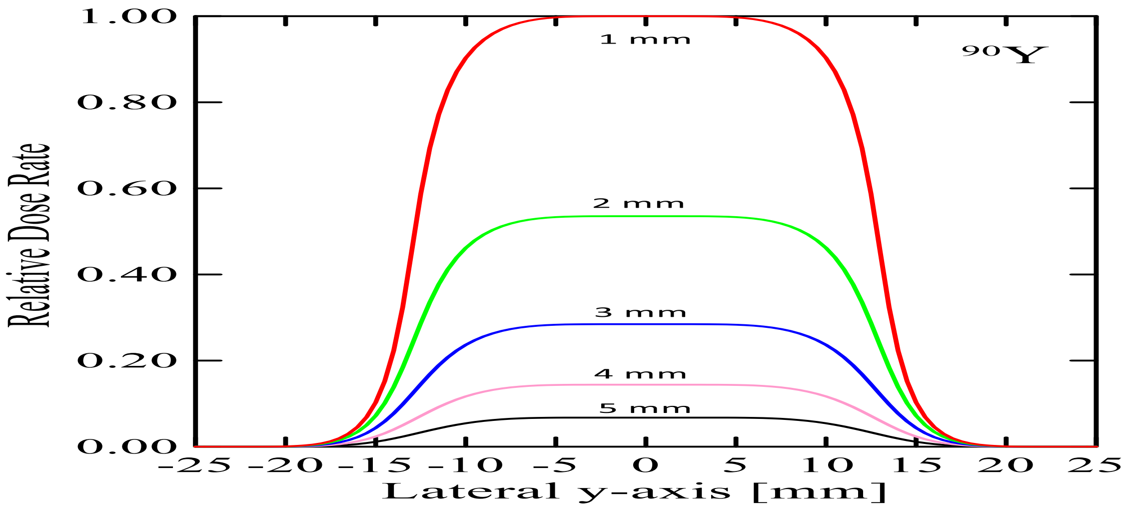

Figure 4. Relative lateral dose rates along *y*-axis for the multi-hexagonal Yttrium-90 beta applicator at 1-, 2-, 3-, 4- and 5-mm depths.

In Figure 5 are depicted the isodoses in the *xy*-plane at the 1 mm depth from the surface of applicator. It is shown the 100%, 80%, 60%, 40%, and 20% isodoses, from the central axis to the direction of applicator edge. Once again, we can note the decrease of doses at farter distances from the central axis.

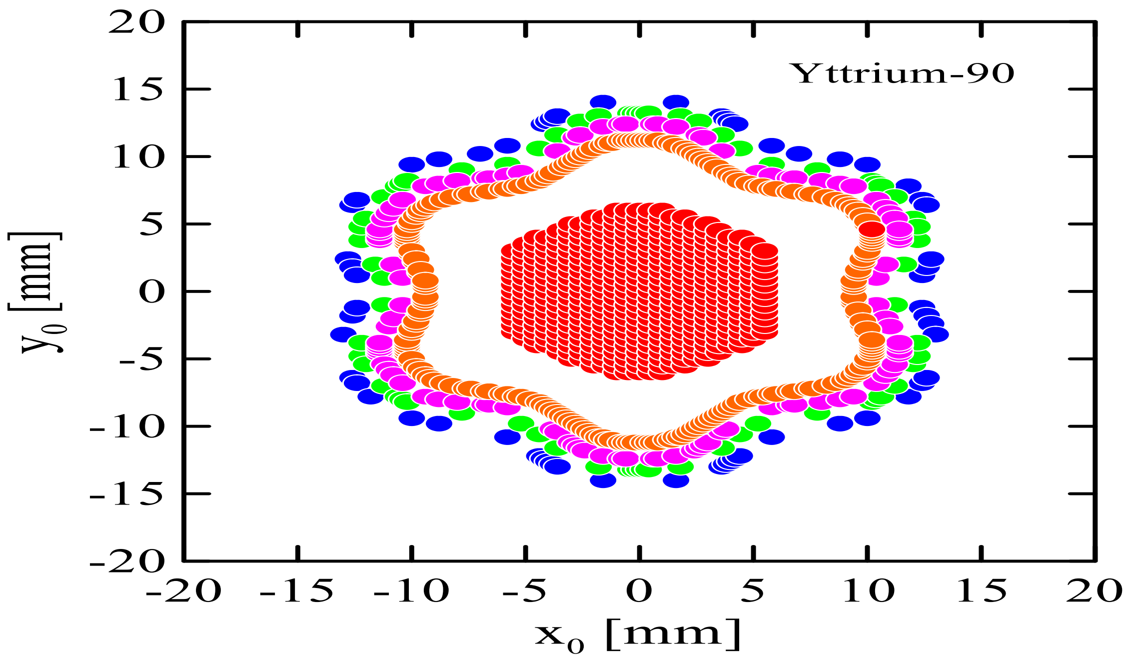

Figure 5. ***xy*-plane dose rates distributions for the multi-hexagonal Yttrium-90 beta applicator at 1 mm depth. Blue color stands for 20% isodose, green for 40%, pink for 60%, orange for 80%, and red for 100% isodose. (To distinguish among colors, the reader should refer to the web version of this work).**

CONCLUSION

In this short note dose rate calculations around a multi-hexagonal conformal beta applicator are presented. Results were obtained using the beta-point source dose function approach and a numerical routine calculation written in Fortran language was developed. Findings show that the multi-hexagonal beta applicator may be suitable to brachytherapy treatment of superficial skin tumors, mainly non-melanomas. In this simple work we choose a multi-hexagonal Yttrium-90 beta applicator of sides equal to 0.5 cm. For a different size of the beta applicator and/or a different radionuclide is straight forward to make the changes within the Fortran code and re-run it. In addition, the increasing ease of 3D printing can be used to construct the applicator opening up the possibility of personalized treatments. Finally, the preliminary results shown here may serve as a first guide to future experimental dosimetry and/or theoretical calculations of dose rates around the multi-hexagonal beta applicator, including Monte Carlo calculations.

REFERENCES

I. Muzic JG, Schmitt AR, Wright AC, et al. Incidence and trends of basal cell carcinoma and cutaneous squamous cell carcinoma: A population-based study in Olmsted County, Minnesota, 2000 to 2010. Mayo Clinic Proceedings 2017; 92: 890-898.

II. Ferry AM, Sarrami, SM, Hollier PC, Thornton JF. Treatment of non-melanoma skin cancers in the absence of Mohs microsurgery. Plastic and Reconstructive Surgery - Global open 2020; 8: e3300.

III. Pashazadeh A, Castro N, Morganti E, et al. Conceptual design of a personalized radiation therapy patch for skin cancer. Current Directions in Biomedical Engineering 2018; 4: 607-610.

IV. Chmura J, Erdman A, Ehler E, et al. Novel design and development of a 3D printed conformal superficial brachytherapy device for the treatment of non-melanoma skin cancer and keloids. 3D Printing in Medicine 2019; 5: 1-6.

V. Pashazadeh A, Landes R, Boese A, et al. Superficial skin cancer therapy with Y-90 microspheres: A feasibility study on patch preparation. Skin Research and Technology 2020; 26: 25-29.

VI. Pashazadeh A, Robatjazi M, Castro NJ, Friebe M. A multiwell applicator for conformal brachytherapy of superficial skin tumors: A simulation study. Skin Research and Technology 2020; 26: 537-541.

VII. Pashazadeh A, De Paiva E, Mahmoodiana N, Friebe M. Calculation of beta radiation dose of a circular Y-90 skin patch: Analytical and simulation methods. Radiation Physics and Chemistry 2020; 166: 108491.

VIII. Rogers B, Lawrence J, Chmra J, et al. Dosimetric characterization of a novel 90Y source for use in the conformal superficial brachytherapy device. Physica Medica 2020; 72: 52-59.

IX. De Paiva E, Pashazadeh A, Robatjazi M. Calculations of beta radiation doses from multiwell Phosphorus-32 and Yttrium-90 applicators designed to be used in the treatment of superficial skin tumors: comparison of Monte Carlo and analytical methods. The European Physical Journal Plus 2022; 137: 916.

X. Yosefof E, Kurman N, and Yaniv D. The role of radiation therapy in the treatment of non-melanoma skin cancer. Cancers 2023; 15: 2408.

XI. De Paiva E. Role of the use of conformal beta applicators in the radiation treatment of small skin lesions. Radiology and Imaging Journal 2023; 2: 1-3.

XII. De Paiva E. A conceptual design of a novel hexagonal beta applicator intended to be used in the treatment of non-melanoma skin cancers. European Chemical Bulletin 2023; 12: 9307-9317.

XIII. McMahon JM. The long-term effect of experimental beta-radiation therapy on the human cornea. Contact Lens and Anterior Eye 2017; 30(4): 249-253.

XIV. Klaassen NJM, Arntz MJ, Arranja AG, et al. The various therapeutic applications of the medical isotope holmium-166: a narrative review. EJNMMI Radiopharmacy and Chemistry 2019; 4: 19.

XV. De Paiva E. Estimates of relative beta radiation doses on central and lateral axes of ruthenium/rhodium COB-type plaque used in eye brachytherapy. Applied Radiation and Isotopes 2020; 156: 108991.

XVI. Radhoe SP, Schuurman AS, Ligthart JM, et al. Two decades after coronary radiation therapy: A single center longitudinal clinical study. Catheterization and Cardiovascular Interventions 2020; 96(3): E204-E212.

XVII. Arora S, Stea BD, Hamilton RJ, Chhablani J. Brachytherapy for Central Serous Chorioretinopathy. Ophthalmology and Therapy 2022; 5: 1611-1616.

XVIII. Diaz MJ, Kwak SH, Root KT, et al. Current Approaches to Craniopharyngioma Management. Frontiers in Bioscience 2022; 27(12): 328.

XIX. Kunikowska J, Morgenstern A, Pelka K, et al. Targeted alpha therapy for glioblastoma. Frontiers in Medicine 2022; 9: 1085245.

XX. Loevinger R. The dosimetry of beta sources in tissue. The point-source function. Radiology 1956; 66: 55-62.

XXI. Vynckier S, Wambersie A. Dosimetry of beta sources in radiotherapy. I. The beta point source dose function. Physics in Medicine and Biology 1982; 27: 1339-1347.

XXII. Vynckier S, Wambersie A. Dosimetry of beta sources in radiotherapy: absorbed dose distributions around plane sources. Radiation Protection. Dosimetry 1986; 14: 169-173.